

# Strong but Simple Baseline with Dual-Granularity Triplet Loss for Visible-Thermal Person Re-Identification

Haijun Liu, Yanxia Chai, Xiaoheng Tan, Dong Li and Xichuan Zhou

**Abstract**—In this letter, we propose a conceptually simple and effective dual-granularity triplet loss for visible-thermal person re-identification (VT-ReID). In general, ReID models are always trained with the sample-based triplet loss and identification loss from the fine granularity level. It is possible when a center-based loss is introduced to encourage the intra-class compactness and inter-class discrimination from the coarse granularity level. Our proposed dual-granularity triplet loss well organizes the sample-based triplet loss and center-based triplet loss in a hierarchical fine to coarse granularity manner, just with some simple configurations of typical operations, such as pooling and batch normalization. Experiments on RegDB and SYSU-MM01 datasets show that with only the global features our dual-granularity triplet loss can improve the VT-ReID performance by a significant margin. It can be a strong VT-ReID baseline to boost future research with high quality.

**Index Terms**—Visible-thermal person re-identification, dual-granularity triplet loss, fine to coarse granularity.

## I. INTRODUCTION

**V**ISIBLE-thermal person re-identification (VT-ReID) is a cross-modality problem and widely encountered in practical scenarios, a 24-hour intelligent surveillance system [18]. Compared to visible-visible ReID (VV-ReID), which focuses on searching a person of interest from multi-disjoint RGB cameras deployed at different locations [6], [20], VT-ReID is a more challenge task, since person images are from different modalities. Apart from the intra-modality (intra- and inter-class) variations as existed in VV-ReID, VT-ReID additionally suffers from the large cross-modality discrepancy, arisen from the different reflective visible spectra and sensed emissivities of visible and thermal (or infrared) cameras.

Recently, an increasing number of researchers have concentrated on the VT-ReID task, achieving substantial progresses with some novel and effective modules and training strategies [7]. However, many works evaluated the effectiveness of their proposed approaches with a poor baseline, which may seriously impede the development of VT-ReID community, since the improvement of baseline model plays an important role. **Therefore, in the present study, we focus on developing a strong and effective baseline for VT-ReID with some simple and typical means.**

Generally, to simultaneously address the intra-modality variations and cross-modality discrepancy, different methods have

been proposed, mainly focusing on the following two aspects: 1) model design and 2) metric learning.

To alleviate the extra cross-modality discrepancy, a two-stream framework is always adopted, including two modality-specific networks with independent parameters for feature extraction, and a parameter-shared network for feature embedding. In the literature, the ResNet50 [3] model is preferentially adopted as the backbone to construct the two-stream network, all the res-convolution blocks for feature extraction and some parameter-shared fully connected layers for feature embedding. In addition, the network is always trained with identification loss and triplet loss to simultaneously enlarge the inter-class distance and encourage the intra-class compactness.

In order to achieve great performance, researchers in the academia always aggregate several part (local) features [14] or leverage semantic information from pose estimation [12]. However, such approaches are not the preferable choice for industry, always bringing extra consumption. In our previous study [8], we have explored how to build the two-stream network and proposed the hetero-center based triplet loss under the part person feature learning framework. **Therefore, in this letter we try to adopt some simple and typical means to improve the capability of the ReID model and only use the global features extracted by the backbone model.**

This letter mainly focuses on the design of an effective baseline from two aspects. On one hand, some simple and typical means are experimentally explored to obtain the global features, including the pooling and batch normalization operations. On the other hand, the organization manner of sample-based triplet loss and center-based triplet loss are also experimentally explored to guide the network training. To summarize, our dual-granularity triplet loss (DGTL), in a hierarchical fine to coarse granularity manner, could achieve superior performance on RegDB [10] and SYSU-MM01 [16] datasets, respectively. It can be a new baseline for VT-ReID with only the global features, through a simple but effective strategy.

## II. DUAL-GRANULARITY TRIPLET LOSS BASED FRAMEWORK

In this section, we introduce the framework of our proposed baseline model for VT-ReID, as depicted in Fig. 1. The framework mainly consists of two components: (1) the two-stream backbone network, and (2) the dual-granularity triplet loss module.

H. Liu, Y. Chai, X. Tan, D. Li and X. Zhou are with the School of Microelectronics and Communication Engineering, Chongqing University, Chongqing, 400044, China.

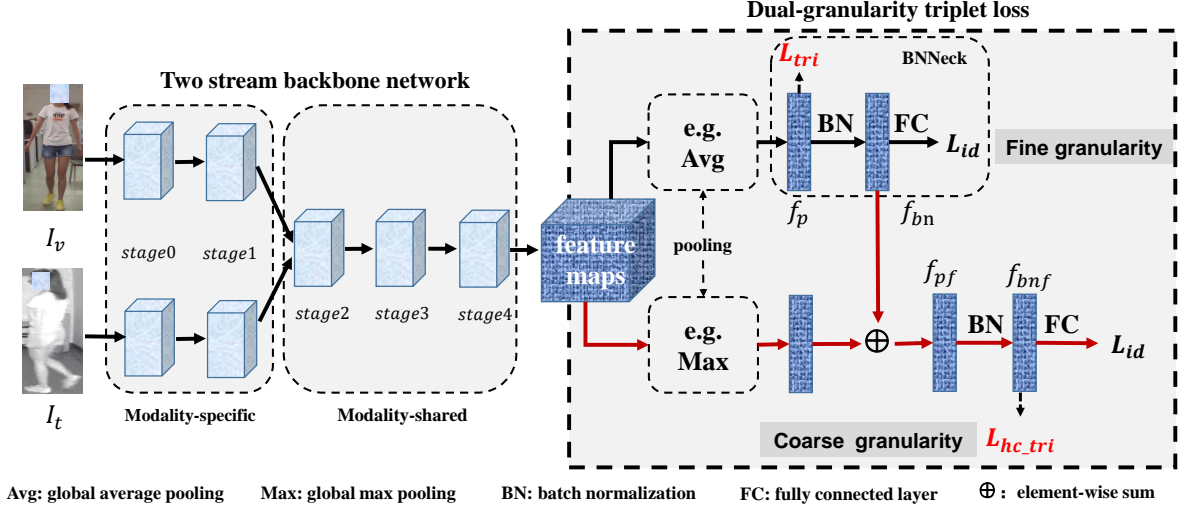


Fig. 1. The pipeline of our proposed framework for VT-ReID, which mainly contains two components: two-stream backbone network and dual-granularity triplet loss module. The two-stream backbone network includes two modality-specific branches with independent parameters and follows one modality-shared branch with shared parameters. Then, the feature maps outputted from the backbone are respectively processed by two pooling methods in the fine granularity branch and coarse granularity branch, with the supervision of our dual-granularity triplet loss. In fine granularity branch, the pooling features are supervised by the sample-based triplet loss ( $L_{tri}$ ) and identification loss ( $L_{id}$ ) with BNNeck [9] to obtain features  $f_{bn}$ , following the black lines (our baseline). Meanwhile, in the coarse granularity branch, the pooling features are firstly fused with  $f_{bn}$ . Afterward, the fused features are supervised by the center-based triplet loss ( $L_{hc\_tri}$ ) and identification loss ( $L_{id}$ ) from the coarse granularity level to obtain features  $f_{bnf}$ , following the additional red lines. During testing, the  $f_{bn}$  and  $f_{bnf}$  with L2 normalization can be adopted as the person features.

#### A. Two-stream backbone network

Based on the observation of our previous study [8], we empirically set the two-stream backbone network as Fig. 1. The ResNet50 [3] model is preferentially adopted as the backbone to construct the two-stream network. The shallow convolution block ( $stage0$ ) and the first res-convolution block ( $stage1$ ) are set as the modality-specific modules with independent parameters to learn the modality-specific 3D information from two heterogeneous modalities. Then the remaining 3 res-convolution blocks ( $stage2$ ,  $stage3$  and  $stage4$ ) are set as the modality-shared module with shared parameters to learn the multi-modality shared feature maps for cross-modality re-identification by projecting those modality-specific feature maps into a modality-shared common 3D feature space.

#### B. Dual-granularity triplet loss module

In this module, there are three aspects should be well studied, 1) the pooling methods, 2) the batch normalization neck and 3) loss function.

1) *Pooling methods*: After obtaining the 3D person feature maps from the two-stream backbone network, we should firstly translate them into 1D feature vectors. We experimentally study three kinds of the pooling methods, the global average pooling (Avg), the global max pooling (Max) and the generalized-mean pooling (GeM) [11].<sup>1</sup>

2) *Batch normalization neck*: The batch normalization neck (BNNeck) [9] is firstly introduced in VV-ReID to address the inconsistent problem of identification and metric losses in the same embedding space. Namely, the metric loss and

identification loss should process different feature vectors, before or after the batch normalization layer. However, in our framework, the BNNeck is only applied in the fine granularity branch, while in the coarse granularity branch the metric and identification losses are both applied to the features after the batch normalization layer ( $f_{bnf}$ ), as shown in Fig. 1.

3) *Dual-granularity triplet loss*: Our previous study [8] only concentrates on the center-based triplet loss, which is in the coarse granularity level. Here, we simultaneously consider the sample-based triplet loss and center-based triplet loss by constructing two branches, and arrange them in a hierarchical fine to coarse granularity manner. One branch focuses on the fine granularity level with sample-based triplet loss ( $L_{tri}$ ) and identification loss ( $L_{id}$ ) (our baseline). The other branch processes the fused features, focusing on the coarse granularity level with center-based triplet loss ( $L_{hc\_tri}$ ) and identification loss ( $L_{id}$ ).

**Batch sampling method**:  $P$  person identities are first randomly selected at each iteration, and then we randomly select  $K$  visible images and  $K$  thermal images of the selected identity to form the mini-batch, in which a total of  $2 * PK$  images are obtained.

**Triplet loss**: For each sample  $x_a$  in the mini-batch, we can select the hardest positive and hardest negative samples within the mini-batch to form the triplets for computing the triplet loss,

$$L_{tri}(X) = \sum_{i=1}^P \sum_{a=1}^{2K} \left[ m + \max_{p=1 \dots 2K} \|x_a^i - x_p^i\|_2 - \min_{\substack{j=1 \dots P \\ n=1 \dots 2K \\ j \neq i}} \|x_a^i - x_n^j\|_2 \right]_+ \quad (1)$$

<sup>1</sup>When the pooling methods in fine and coarse branches are identical (as experimentally set for RegDB dataset), the two branches degenerate to one with a feature skip connection across the batch normalization layer.

which is defined for a mini-batch  $X$ , where a data point  $x_a^i$  denotes the  $a^{th}$  image feature of the  $i^{th}$  person in the batch,  $[x]_+ = \max(x, 0)$  denotes the standard hinge loss,  $\|x_a - x_p\|_2$  denotes the Euclidean distance of data point  $x_a$  and  $x_p$ ,  $m$  is the margin.

**Hetero-center triplet loss:** First, in a mini-batch, the feature centers of every identity from each modality are computed,  $c_v^i = \frac{1}{K} \sum_{j=1}^K v_j^i$ ,  $c_t^i = \frac{1}{K} \sum_{j=1}^K t_j^i$ , which is defined for a mini-batch, where  $v_j^i$  denotes the  $j^{th}$  visible image feature of the  $i^{th}$  person in the mini-batch, while  $t_j^i$  corresponds to the thermal image feature. Then, in our VT-ReID, based on the  $PK$  sampling strategy and calculated centers, we can define the hetero-center triplet loss as,

$$L_{hc\_tri}(C) = \sum_{i=1}^P \left[ mc + \|c_v^i - c_t^i\|_2 - \min_{\substack{n \in \{v,t\} \\ j \neq i}} \|c_v^i - c_n^j\|_2 \right]_+ + \sum_{i=1}^P \left[ mc + \|c_t^i - c_v^i\|_2 - \min_{\substack{n \in \{v,t\} \\ j \neq i}} \|c_t^i - c_n^j\|_2 \right]_+, \quad (2)$$

which is defined on mini-batch centers  $C$  including both visible centers  $\{c_v^i | i = 1, \dots, P\}$  and thermal centers  $\{c_t^i | i = 1, \dots, P\}$ ,  $mc$  is the margin. For each identity,  $L_{hc\_tri}$  concentrates on only one cross-modality positive pair and the mined hardest negative pair in both the intra- and inter-modality.

Finally, the dual-granularity triplet loss is,

$$L_{all} = \underbrace{L_{tri}(f_p) + L_{id}(f_{bn})}_{\text{fine granularity}} + \underbrace{L_{hc\_tri}(f_{bnf}) + L_{id}(f_{bnf})}_{\text{coarse granularity}}, \quad (3)$$

where  $f_p$ ,  $f_{bn}$  and  $f_{bnf}$  are the person features as shown in Fig. 1.

### III. EXPERIMENTS

We evaluate the effectiveness of our proposed method for VT Re-ID tasks on two public datasets, RegDB [10] and SYSU-MM01 [16]. The implementation<sup>2</sup> of our method is with the Pytorch framework. The training and testing procedures are following the official settings as done in [8], [20]. For the  $PK$  sampling strategy, we set  $P = 8$ ,  $K = 4$  for the RegDB, and  $P = 6$ ,  $K = 8$  for the SYSU-MM01. The pooling method is Max in both fine and coarse branches for RegDB, while Avg in fine branch and Max in coarse branch for SYSU-MM01. We set  $m = 0.3$ ,  $mc = 0.3$  for RegDB, and  $mc = 0.8$  for SYSU-MM01. The fusion method is element-wise sum.

#### A. Comparison to the state-of-the-art

In this section, our DGTL with only the global features is compared to some state-of-the-art VT-ReID methods, recently published in 2020. The results on the RegDB and SYSU-MM01 datasets are listed in Tables I and II, respectively.<sup>3</sup>

<sup>2</sup><https://github.com/hijune6/DGTL-for-VT-ReID>

<sup>3</sup>Note that in this subsection, we reported the mean results of 10 trials following the standard dataset settings.

TABLE I  
COMPARISON TO THE STATE-OF-THE-ART METHODS ON THE REGDB DATASETS. RE-IDENTIFICATION RATES AT RANK1 AND MAP (%).

Methods	Venue	Visible to Thermal		Thermal to Visible	
		rank1	mAP	rank1	mAP
CMSP [15]	IJCV20	65.07	64.50	-	-
HAT [21]	TIFS20	71.83	67.56	70.02	66.30
MSR [2]	TIP20	48.43	48.67	-	-
MACE [17]	TIP20	72.37	69.09	72.12	68.57
Hi-CMD [1]	CVPR20	70.93	66.04	-	-
CML [5]	MM20	59.81	60.86	-	-
JSIA [13]	AAAI20	48.10	48.90	48.50	49.30
XIV [4]	AAAI20	62.21	60.18	-	-
DDAG [19]	ECCV20	69.34	63.46	68.06	61.08
DGTL $f_{bn}$	ours	83.56	73.36	81.27	71.22
DGTL $f_{bnf}$		<b>83.92</b>	<b>73.78</b>	<b>81.59</b>	<b>71.65</b>
HcTri [8]	TMM20	91.05	83.28	89.30	81.46

TABLE II  
COMPARISON TO THE STATE-OF-THE-ART METHODS ON THE SYSU-MM01 DATASETS. RE-IDENTIFICATION RATES AT RANK1 AND MAP (%).

Methods	Venue	All search		Indoor search	
		rank1	mAP	rank1	mAP
CMSP [15]	IJCV20	43.56	44.98	48.62	57.50
HAT [21]	TIFS20	55.29	53.89	62.10	69.37
MSR [2]	TIP20	37.35	38.11	39.64	50.88
MACE [17]	TIP20	51.64	50.11	57.35	64.79
Hi-CMD [1]	CVPR20	34.94	35.94	-	-
CML [5]	MM20	51.80	51.21	54.98	63.7
JSIA [13]	AAAI20	38.10	36.90	43.80	52.90
XIV [4]	AAAI20	49.92	50.73	-	-
DDAG [19]	ECCV20	54.75	53.02	61.02	67.98
DGTL $f_{bn}$	ours	54.66	52.72	59.21	66.27
DGTL $f_{bnf}$		<b>57.34</b>	<b>55.13</b>	<b>63.11</b>	<b>69.20</b>
HcTri [8]	TMM20	61.68	57.51	63.41	68.17

They show that our proposed DGTL method can achieve much better performance, especially compared to those methods with only the global features (CMSP [15], HAT [21], MSR [2], MACE [17], Hi-CMD [1], CML [5], JSIA [13] and XIV [4]), even outperforming the DDAG [19] method, which adopts the part-aggregated feature learning to refine the person features. Moreover, the results based on the  $f_{bn}$  feature, just the direct output of the ResNet50 model, also can achieve satisfactory performance, even similar to those results based on  $f_{bnf}$  feature on RegDB dataset. It demonstrates the effectiveness of our dual-granularity triplet loss module with a simple but effective strategy, which truly can be a strong VT-ReID baseline to boost future research with high quality.

Our DGTL method performs worse than HcTri [8], which is our previous study for part feature learning with much more model parameters and training tricks.

#### B. Ablation experiments

We evaluate the effectiveness of our proposed DGTL module, including three components, pooling methods, loss functions organization and the BNNeck configuration.<sup>4</sup>

<sup>4</sup>Note that to simply show the effectiveness of different components, during the ablation experiments, we only reported one trial experimental results, rather than the mean results of 10 trials.

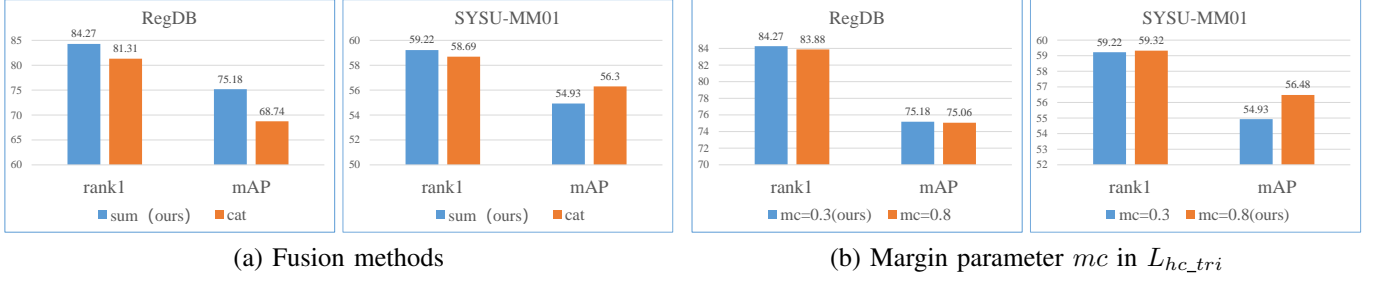


Fig. 2. The effects of (a) fusion methods (sum: element-wise sum, cat: concatenation) and (b) margin parameter  $mc$  in  $L_{hc\_tri}$  on RegDB and SYSU-MM01 datasets. Re-identification rates of rank1 and mAP (%).

TABLE III

THE EFFECTS OF DIFFERENT POOLING METHODS IN BASELINE NETWORK (THE FINE GRANULARITY BRANCH). RE-IDENTIFICATION RATES OF RANK1 AND MAP (%).

	RegDB		SYSU-MM01	
	rank1	mAP	rank1	mAP
Avg	70.63	65.13	<b>58.66</b>	<b>54.57</b>
Max	<b>80.49</b>	<b>71.23</b>	49.04	47.35
GeM	75.39	67.72	55.85	53.25

TABLE IV

THE EFFECTS OF DIFFERENT POOLING METHODS IN THE COARSE GRANULARITY BRANCH. THE POOLING METHOD IN FINE GRANULARITY BRANCH IS MAX FOR REGDB DATASET AND AVG FOR SYSU-MM01 DATASET. RE-IDENTIFICATION RATES OF RANK1 AND MAP (%).

RegDB				
Fine	Coarse	features	rank1	mAP
Max	Avg	$f_{bn}$	83.59	72.08
		$f_{bnf}$	83.30	72.13
	Max	$f_{bn}$	83.64	74.53
		$f_{bnf}$	<b>84.27</b>	<b>75.18</b>
	GeM	$f_{bn}$	77.82	68.59
		$f_{bnf}$	77.28	68.17
SYSU-MM01				
Avg	Avg	$f_{bn}$	56.59	54.02
		$f_{bnf}$	56.74	54.23
	Max	$f_{bn}$	55.35	52.44
		$f_{bnf}$	<b>59.22</b>	54.93
	GeM	$f_{bn}$	56.22	53.98
		$f_{bnf}$	57.67	<b>55.14</b>

Table III and IV list the results of different pooling methods organizing in fine and coarse granularity branches, respectively. Different pooling methods truly perform differently, always with large gaps (Avg vs. Max: 70.63 vs. 80.49, rank1 on regdb dataset). Therefore, the pooling method is a key factor for constructing the VT-ReID baseline.

Table V lists the results of different triplet losses organization in the fine and coarse granularity branches. In our baseline methods (only with the fine granularity branch), the combination of  $L_{tri}$  and  $L_{hc\_tri}$  truly can improve the VT-ReID performance. As to the dual-granularity setting, the arrangements of  $L_{tri}$  and  $L_{hc\_tri}$  have impact on the performance. In summary, our proposed hierarchical fine to coarse (f2c) granularity manner could obtain the best performance.

Table VI shows that the BNNeck [9] module only applied in the fine granularity branch is the best setting. Moreover, Fig. 2 also illustrates the effects of different fusion methods

TABLE V

THE ABLATION STUDY OF TRIPLET LOSSES ORGANIZING IN THE FINE AND COARSE GRANULARITY BRANCHES, HETERO-CENTER TRIPLET LOSS ( $L_{hc\_tri}$ ) AND SAMPLE-BASED TRIPLET LOSS ( $L_{tri}$ ). RE-IDENTIFICATION RATES OF RANK1 AND MAP (%).

index	Fine		Coarse	features	RegDB		SYSU-MM01	
					rank1	mAP	rank1	mAP
①	$L_{tri}$	$L_{hc\_tri}$	×	$f_{bn}$	80.49	71.23	58.66	54.57
②	$L_{tri}$	$L_{hc\_tri}$	×	$f_{bn}$	80.58	65.57	53.22	50.34
③	$L_{tri}$	$L_{hc\_tri}$	×	$f_{bn}$	83.74	74.81	57.95	55.48
f2f	$L_{tri}$	$L_{tri}$	$f_{bn}$	$f_{bnf}$	80.78	72.09	53.75	50.45
			78.16	71.36	78.16	71.36	57.51	54.70
c2c	$L_{hc\_tri}$	$L_{hc\_tri}$	$f_{bn}$	$f_{bnf}$	81.70	66.65	54.72	50.64
			82.33	66.68	82.33	66.68	57.45	53.44
c2f	$L_{hc\_tri}$	$L_{tri}$	$f_{bn}$	$f_{bnf}$	80.53	72.90	53.88	51.16
			78.74	72.58	78.74	72.58	57.53	55.82
f2c	$L_{tri}$	$L_{hc\_tri}$	$f_{bn}$	$f_{bnf}$	83.64	74.53	55.96	53.85
			<b>84.27</b>	<b>75.18</b>	<b>84.27</b>	<b>75.18</b>	<b>59.32</b>	<b>56.48</b>

TABLE VI

THE ABLATION STUDY OF BNNECK [9] IN THE FINE AND COARSE GRANULARITY BRANCHES. WHETHER APPLYING THE BNNECK OR NOT, I.E., WHERE THE TRIPLET LOSS SHOULD BE ADOPTED, FOR THE POOL FEATURES ( $f_p, f_{pf}$ ) OR THE BATCH NORMALIZATION FEATURES ( $f_{bn}, f_{bnf}$ )? RE-IDENTIFICATION RATES OF RANK1 AND MAP (%).

		RegDB		SYSU-MM01	
Fine	Coarse	rank1	mAP	rank1	mAP
$L_{tri}$	$L_{hc\_tri}$				
$f_p$	×	80.49	71.23	58.66	54.57
$f_{bn}$	×	77.43	70.53	49.78	48.99
$f_p$	$f_{pf}$	75.97	66.52	58.37	54.49
$f_{bn}$	$f_{bnf}$	81.17	72.57	54.77	52.42
$f_p$	$f_{bnf}$	<b>84.27</b>	<b>75.18</b>	<b>59.32</b>	<b>56.48</b>

and the margin parameter in  $L_{hc\_tri}$ .

The best performances for two datasets are with different configurations. The reason may lie in the image conditions. For RegDB, the visible and corresponding thermal images are well aligned. While for SYSU-MM01, the visible and corresponding infrared images have arbitrary poses and views.

#### IV. CONCLUSIONS

In this study, we propose a strong baseline for VT-ReID with a simple but effective strategy. To our best knowledge, it can achieve the best performance with only the global features of a single backbone. Our proposed DGTL method arranges the sample-based triplet loss and center-based triplet loss in a hierarchical fine to coarse granularity manner. Some simple configurations of typical operations, especially the pooling methods and batch normalization, are also explored for VT-ReID tasks. We hope that this study can promote the VT-ReID research with high quality.

## REFERENCES

- [1] S. Choi, S. Lee, Y. Kim, T. Kim, and C. Kim, “Hi-cmd: Hierarchical cross-modality disentanglement for visible-infrared person re-identification,” in *CVPR*, 2020, pp. 10 257–10 266.
- [2] Z. Feng, J. Lai, and X. Xie, “Learning modality-specific representations for visible-infrared person re-identification,” *IEEE TIP*, vol. 29, pp. 579–590, 2020.
- [3] K. He, X. Zhang, S. Ren, and J. Sun, “Deep residual learning for image recognition,” in *CVPR*, 2016, pp. 770–778.
- [4] D. Li, X. Wei, X. Hong, and Y. Gong, “Infrared-visible cross-modal person re-identification with an x modality,” in *AAAI*, 2020, pp. 4610–4617.
- [5] Y. Ling, Z. Zhong, Z. Luo, P. Rota, S. Li, and N. Sebe, “Class-aware modality mix and center-guided metric learning for visible-thermal person re-identification,” in *ACM MM*, 2020, pp. 889–897.
- [6] H. Liu and J. Cheng, “Gallery based k-reciprocal-like re-ranking for heavy cross-camera discrepancy in person re-identification,” *Neurocomputing*, vol. 333, pp. 64–75, 2019.
- [7] H. Liu, J. Cheng, W. Wang, Y. Su, and H. Bai, “Enhancing the discriminative feature learning for visible-thermal cross-modality person re-identification,” *Neurocomputing*, vol. 398, pp. 11–19, 2020.
- [8] H. Liu, X. Tan, and X. Zhou, “Parameter sharing exploration and hetero-center triplet loss for visible-thermal person re-identification,” *IEEE TMM*, pp. 1–1, 2020.
- [9] H. Luo, W. Jiang, Y. Gu, F. Liu, X. Liao, S. Lai, and J. Gu, “A strong baseline and batch normalization neck for deep person re-identification,” *IEEE TMM*, vol. 22, no. 10, pp. 2597–2609, 2020.
- [10] D. Nguyen, H. Hong, K. Kim, and K. Park, “Person recognition system based on a combination of body images from visible light and thermal cameras,” *Sensors*, vol. 17, no. 3, p. 605, 2017.
- [11] F. Radenović, G. Tolias, and O. Chum, “Fine-tuning cnn image retrieval with no human annotation,” *IEEE TPAMI*, vol. 41, no. 7, pp. 1655–1668, 2018.
- [12] C. Su, J. Li, S. Zhang, J. Xing, W. Gao, and Q. Tian, “Pose-driven deep convolutional model for person re-identification,” in *ICCV*, 2017, pp. 3980–3989.
- [13] G. Wang, T. Zhang, Y. Yang, J. Cheng, J. Chang, X. Liang, and Z. Hou, “Cross-modality paired-images generation for rgb-infrared person re-identification,” in *AAAI*, 2020, pp. 12 144–12 151.
- [14] P. Wang, Z. Zhao, F. Su, Y. Zhao, H. Wang, L. Yang, and Y. Li, “Deep multi-patch matching network for visible thermal person re-identification,” *IEEE TMM*, pp. 1–1, 2020.
- [15] A. Wu, W.-S. Zheng, S. Gong, and J. Lai, “Rgb-ir person re-identification by cross-modality similarity preservation,” *IJCV*, vol. 128, pp. 1765–1785, 2020.
- [16] A. Wu, W. Zheng, H. Yu, S. Gong, and J. Lai, “Rgb-infrared cross-modality person re-identification,” in *ICCV*, 2017, pp. 5380–5389.
- [17] M. Ye, X. Lan, and Q. Leng, “Cross-modality person re-identification via modality-aware collaborative ensemble learning,” *IEEE TIP*, vol. 29, pp. 9387–9399, 2020.
- [18] M. Ye, X. Lan, Z. Wang, and P. C. Yuen, “Bi-directional center-constrained top-ranking for visible thermal person re-identification,” *IEEE TIFS*, vol. 15, pp. 407–419, 2020.
- [19] M. Ye, J. Shen, D. J. Crandall, L. Shao, and J. Luo, “Dynamic dual-attentive aggregation learning for visible-infrared person re-identification,” in *ECCV*, 2020.
- [20] M. Ye, J. Shen, G. Lin, T. Xiang, L. Shao, and S. C. H. Hoi, “Deep learning for person re-identification: A survey and outlook,” *arXiv preprint arXiv:2001.04193*, 2020.
- [21] M. Ye, J. Shen, and L. Shao, “Visible-infrared person re-identification via homogeneous augmented tri-modal learning,” *IEEE TIFS*, vol. 16, pp. 728–739, 2021.